Diameter Dependence of the Dielectric Constant for the Excitonic Transition Energy of Single-Wall Carbon Nanotubes

P. T. Araujo,[1] A. Jorio,[1,2] M. S. Dresselhaus,[3] K. Sato,[4] and R. Saito[4]

[1]*Departamento de Física, Universidade Federal de Minas Gerais, Belo Horizonte, MG, 30123-970 Brazil*

[2]*Divisão de Metrologia de Materiais, Instituto Nacional de Metrologia, Normalização e Qualidade Industrial (INMETRO), Duque de Caxias, RJ, 25250-020, Brazil*

[3]*Department of Electrical Engineering and Computer Science, and Department of Physics, Massachusetts Institute of Technology, Cambridge, Massachusetts 02139-4307, USA*

[4]*Department of Physics, Tohoku University, Sendai 980-8578, Japan*

(Received 14 April 2009; published 30 September 2009)

The measured optical transition energies E_{ii} of single-wall carbon nanotubes are compared with bright exciton energy calculations. The E_{ii} differences between experiment and theory are minimized by considering a diameter-dependent dielectric constant κ, which comprises the screening from the tube and from the environment. Different κ dependencies are obtained for (E_{11}^S, E_{22}^S, E_{11}^M) relative to (E_{33}^S, E_{44}^S). A changing environment changes the κ diameter dependence for (E_{11}^S, E_{22}^S, E_{11}^M), but for (E_{33}^S, E_{44}^S) the environmental effects are minimal. The resulting calculated exciton energies reproduce experimental E_{ii} values within ± 70 meV for a diameter range ($0.7 < d_t < 3.8$ nm) and $1.2 < E_{ii} < 2.7$ eV, thus providing a theoretical justification for E_{ii}, environmental effects and important insights on the dielectric screening in one-dimensional structures.

DOI: 10.1103/PhysRevLett.103.146802 PACS numbers: 73.22.−f, 61.48.De, 78.20.-e, 78.67.Ch

The last decade has been marked by an impressive development in understanding the nature of the optical transition energies in quasi-one-dimensional single-wall carbon nanotubes (SWNTs) [1], called E_{ii}, where $i = 1, 2, 3, \ldots$ denotes the intersubband transitions between the ith valence and the ith conduction band for a given SWNT. While the interest in excitons and dielectric screening in one-dimensional structures dates from research in π-conjugated polymers, in carbon nanotubes the large attention started in 2003 with the so-called ''ratio problem'' [2]. Strong debate still exists about the strength of the exciton binding energy, mostly related to the complex dielectric screening in one-dimensional materials. In 2007, Araujo *et al.* [3] and Michel *et al.* [4] showed that the scaling law for the exciton energies explaining the ratio problem [2] breaks down for transitions higher than E_{11}^M. These results lead to the discussion of the exciton nature for higher energy levels, where quantum-chemistry calculations and solid-state physics (tight binding and first-principles) calculations give contradictory pictures [3,5]. Now, the accumulated knowledge in SWNTs, both theoretical and experimental [1], makes it possible to evaluate in detail the dielectric screening in one-dimensional systems.

The E_{ii} values are now understood in terms of the bright exciton energy in a framework of a tight binding calculation which includes curvature optimization [1] and many-body effects [1,5,6]. The assignment of E_{ii} for SWNTs over a large region of both diameter ($0.7 < d_t < 3.8$ nm) and E_{ii} (1.2–2.7 eV) values and for a variety of surrounding materials are now available [1], thus making it possible to accurately determine the effect of the general dielectric constant κ on E_{ii}. By ''general'' we mean κ comprises the screening from the tube and from the environment. In this work we show a d_t-dependent effective κ values for the exciton calculation that are needed to reproduce the experimental E_{ii} values consistently. The results thus obtained are important for the physics of quasi and truly one-dimensional materials and can be used in interpreting optical experiments and environment effects.

Figure 1 shows a map of previously reported experimental E_{ii} values (black dots) [7–9] from a SWNT sample grown by the water-assisted (''super-growth'') chemical vapor deposition method [10–13]. The resulting data for the E_{ii} transition energies are plotted as a function of the radial breathing mode frequencies ω_{RBM}, as obtained by resonance Raman spectroscopy (RRS) [7–9,14]. This sample was chosen for the initial analysis developed in this paper because the sample has a homogeneous environment and a large variety of SWNT diameters, as measured by RRS. Furthermore, this sample shows the following features: (i) Experimental observation of the fundamental relation $\omega_{\mathrm{RBM}} = 227/d_t$, for which the constant term B is zero in the relation $\omega_{\mathrm{RBM}} = A/d_t + B$. The constant term B comes from the interaction of SWNTs with their environment, which is negligible for the present low-density SWNT example [7]. (ii) The highest E_{ii} values are obtained for these SWNTs when compared to other samples in the literature [8]. This result indicates that the tubes are surrounded by the lowest environmental dielectric constant ($\kappa_{\mathrm{env}} \rightarrow 1$) reported in the literature [1,3,4,15–21]. (iii) The previously elusive high energy

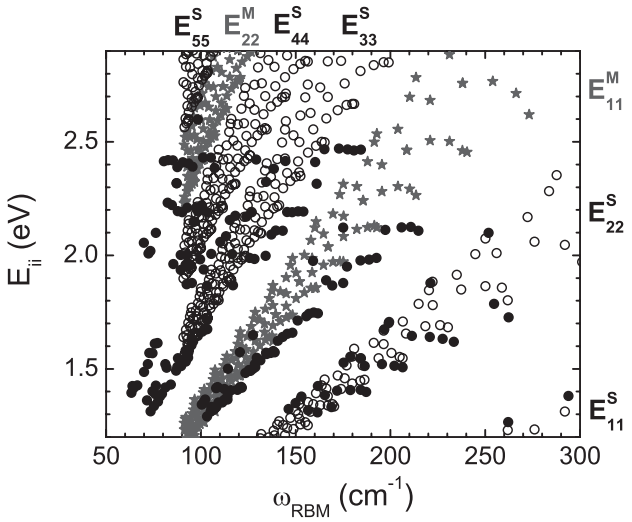

FIG. 1. Black dots show E_{ii}^{exp} vs ω_{RBM} results obtained from resonance Raman spectra taken from the super-growth SWNT sample [7–9]. The black open circles (semiconducting) and the dark-gray stars (metallic) give E_{ii}^{cal} for the bright exciton calculation with dielectric constant $\kappa = 1$ [6]. Along the x axis, the E_{ii}^{cal} points are translated using the relation $\omega_{\mathrm{RBM}} = 227/d_t$ [7]. Due to time consumption, only E_{ii} for tubes with $d_t < 2.5$ nm (i.e., $\omega_{\mathrm{RBM}} > 91$ cm^{-1}) have been calculated. Transition energies E_{ii}^{S} ($i = 1 - 5$) stand for semiconducting and E_{ii}^{M} ($i = 1, 2$) stand for metallic SWNTs.

E_{ii}^{M} transitions [18–20] can be observed for metallic SWNTs in these samples [14], indicating the lowest degree of perturbation for metallic tubes as compared to other samples in the literature. In Fig. 1, the experimental values of E_{ii} vs ω_{RBM} for the super-growth sample E_{ii}^{exp} are compared with the calculated bright exciton energies E_{ii}^{cal} (open circles and stars). Although E_{ii}^{cal} include SWNT curvature and many-body effects [6], clearly the E_{ii}^{exp} values are redshifted when compared with theory, and the redshift depends on ω_{RBM}, i.e., on d_t, and on the optical levels (i in E_{ii}).

The E_{ii} values can be renormalized in the calculation by explicitly considering the dielectric constant κ in the coulomb potential energy $V(q)/\varepsilon(q)\kappa$ [22]. Here, κ represents the screening of the e-h (electron-hole) pair by core ($1s$) and σ electrons (κ_{tube}) and by the surrounding materials (κ_{env}). Here $\varepsilon(q)$ explicitly gives the polarization function for π-electrons calculated within the random phase approximation (RPA) [6,22,23]. To fully account for the observed energy-dependent E_{ii} redshift, we fit the total κ values $(1/\kappa = C_{\mathrm{env}}/\kappa_{\mathrm{env}} + C_{\mathrm{tube}}/\kappa_{\mathrm{tube}})$ to minimize $E_{ii}^{\mathrm{exp}} - E_{ii}^{\mathrm{cal}}$. The bullets in Fig. 2 show the fitted κ values as a function of p/d_t, which reproduce each experimental E_{ii} value for the assigned (n, m) SWNTs for the super-growth SWNT sample. The stars stand for a different SWNT sample, named "alcohol-assisted" SWNTs [24], and they will be discussed below in the next paragraph. The integer p corresponds to the distance ratio of the cutting

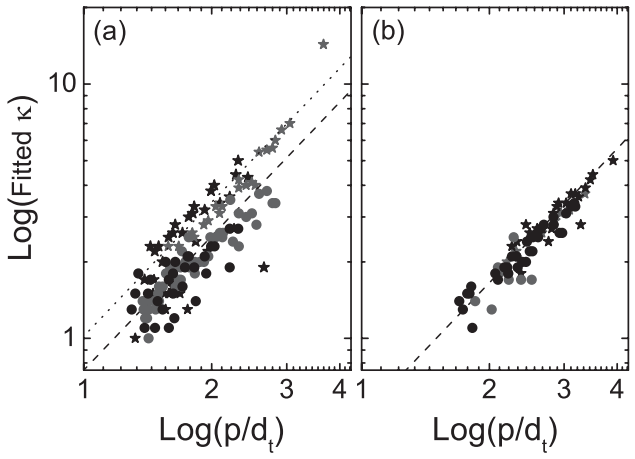

FIG. 2. The calculated κ, which are fitted to the experimental E_{ii} values from the super-growth (bullets) [8,9] and alcohol-assisted (stars) [3,9] samples. (a) E_{22}^{S} (black) and E_{11}^{M} (dark gray). The dashed and dotted curves are given by Eq. (1) with $C_\kappa = 0.75$ and 1.02, respectively. (b) E_{33}^{S} (black) and E_{44}^{S} (dark gray). The dashed curve is for Eq. (1) with $C_\kappa = 0.49$.

lines from the K point, where $p = 1$, 2, 3, 4 and 5 stands for E_{11}^{S}, E_{22}^{S}, E_{11}^{M}, E_{33}^{S}, and E_{44}^{S}, respectively [1]. Thus p/d_t represents the distance of the k point from the K point in the two-dimensional Brillouin zone of graphene. Consideration of p/d_t allows us to compare the κ values of SWNTs with different d_t and different E_{ii} using the same plot. As seen in Fig. 2, the κ values increase with increasing p/d_t for different E_{ii} values. The κ values for E_{33}^{S} and E_{44}^{S} [Fig. 2(b)] appear in a smaller κ region than those for E_{11}^{S} and E_{22}^{S} [Fig. 2(a)].

To gain more insight into the κ influence on the optical transition energies, Fig. 3 shows a comparison between the E_{ii}^{exp} from the super-growth SWNT sample (bullets) [8] and

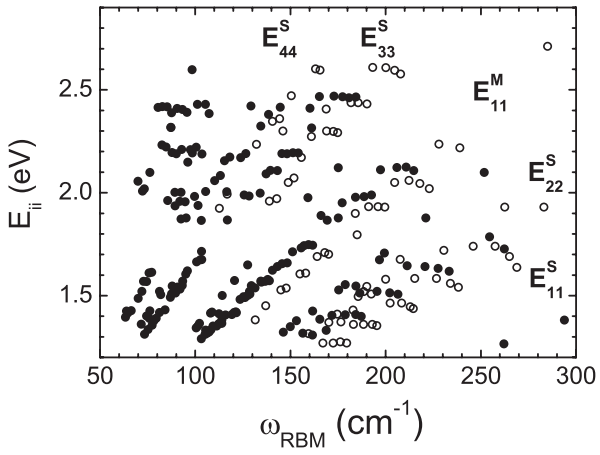

FIG. 3. E_{ii}^{exp} vs ω_{RBM} results obtained for the super-growth (bullets) [8,9] and alcohol assisted (open circles) [3,9] SWNT samples.

from the "alcohol-assisted" SWNT samples (open circles) [3]. The alcohol-assisted SWNT sample is chosen for comparison for three reasons: (i) this sample also has a broad diameter distribution ($0.7 < d_t < 2.3$ nm); (ii) the observed E_{ii} are similar to many other samples in the literature [8]; (iii) the sample is morphologically similar to the super-growth sample (both are carpetlike free standing SWNTs). From Fig. 3, we see that the E_{ii}^{exp} values from the "alcohol-assisted" SWNTs are generally redshifted with respect to those from the super-growth SWNTs. Assuming that κ_{tube} does not change from sample to sample, since the structure of a given (n, m) tube should be the same, these results indicate that the alcohol-assisted SWNTs are surrounded by a larger κ_{env} value, thus increasing the effective κ and decreasing E_{ii}.

Looking at Fig. 2 we can observe the difference in the κ values resulting from fitting the E_{ii}^{exp} to the super-growth (bullets) in comparison to alcohol-assisted (stars) SWNT samples. For E_{22}^S and E_{11}^M [Fig. 2(a)], we see a clear difference for κ up to $p = 3$ when comparing the two samples. However, for E_{33}^S and E_{44}^S [Fig. 2(b)], no difference in κ between the two samples can be seen. This means that the electric field of the E_{33}^S and E_{44}^S excitons do not extend much outside the SWNT volume, in contrast to the E_{22}^S and E_{11}^M excitons for which the κ_{env} effect is significant. Since the effect of κ_{env} is relatively small for energies above E_{11}^M, it is possible to assign the (n, m) values from E_{33}^S and E_{44}^S if the dielectric constant of the environment is not known, even though the E_{33}^S and E_{44}^S values are seen within a large density of dots in the Kataura plot. In constructing Fig. 2, we used the relation

$$\kappa = C_\kappa \left(\frac{p}{d_t}\right)^{1.7}, \tag{1}$$

where the exponent 1.7 was found to work for all E_{ii}^{exp}, but different C_κ parameters are needed. For E_{11}^S, E_{22}^S and E_{11}^M, $C_\kappa = 0.75$ for the super-growth SWNTs and $C_\kappa = 1.02$ for the alcohol-assisted SWNTs (dashed and dotted curves in Fig. 2(a), respectively). The E_{33}^S and E_{44}^S are fitted using $C_\kappa = 0.49$ for both samples, as shown by the dashed line in Fig. 2(b). Figure 4 summarizes the effect of our κ-based renormalization of E_{ii}. In Fig. 4 we plot the energy difference $\Delta E_{ii} = E_{ii}^{\text{exp}} - E_{ii}^{\text{cal}}$ as a function of d_t for (a) κ values fixed to be equal to 1 ($\kappa = 1$), (b) κ values fixed to be equal to 2.22 ($\kappa = 2.22$), broadly used in the literature [1] and (c) the diameter-dependent κ values using the function of Eq. (1), including both the super-growth SWNTs and the alcohol-assisted SWNTs. From Figs. 4(a) and 4(b) we observe that the fitting results using fixed values for κ are not good enough from a physical point of view, because the data in these figures are spread over a window of about 400 meV, which is greater than the observed resonance window for a single (n, m) tube [1]. Besides, the spread of the ΔE_{ii} points in Figs. 4(a) and 4(b) increases for small d_t tubes. To address this physical inconsistency, we analyze

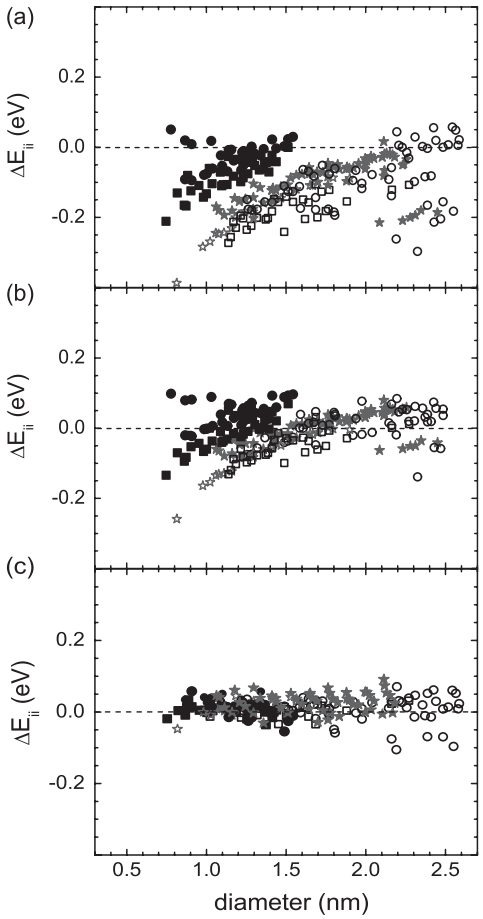

FIG. 4. The difference $\Delta E_{ii} = E_{ii}^{\text{exp}} - E_{ii}^{\text{cal}}$ as a function of d_t for (a) $\kappa = 1$, (b) $\kappa = 2.22$ and (c) the diameter-dependent κ given by Eq. (1). Closed stars (ΔE_{11}^M for metallic tubes), closed bullets (ΔE_{11}^S and ΔE_{22}^S for semiconducting tubes) and open bullets (ΔE_{33}^S and ΔE_{44}^S for semiconducting tubes) stand for super-growth data, while open stars (ΔE_{11}^M for metallic tubes), closed squares (ΔE_{11}^S and ΔE_{22}^S for semiconducting tubes) and open squares (ΔE_{33}^S and ΔE_{44}^S for semiconducting tubes) stand for alcohol-assisted data.

the energy difference $\Delta E_{ii} = E_{ii}^{\text{exp}} - E_{ii}^{\text{cal}}$, where E_{ii}^{cal} is now calculated by considering κ given by Eq. (1). When the resulting ΔE_{ii} is plotted vs d_t for all E_{ii} ($p = 1, \ldots, 5$), using the C_κ parameters given in the text, all the ΔE_{ii} in Fig. 4(c) deviate from zero by less than 70 meV, for both the super-growth and the "water-assisted" SWNT samples, over the entire d_t region.

Qualitatively, the origin of the diameter dependence presented by Eq. (1) consists of: (i) the exciton size and (ii) the amount of electric field "feeling" the dielectric constant of the surrounding material. These two factors are connected and the development of an electromagnetism model is needed to fully rationalize this equation. Interestingly, the similarity between the κ values found for E_{22}^S and E_{11}^M shows that the difference between metallic and semiconducting tubes is satisfactorily accounted by the

RPA in $\varepsilon(q)$ [5]. Also interesting is the different κ behavior observed for higher levels ($p > 3$), where C_κ is smaller than for E_{ii} with $p \leq 3$, and it is independent of the sample environment. Again, two pictures can be given: (1) the more localized exciton wave function (a larger exciton binding energy) for E_{33}^S and E_{44}^S compared with E_{11}^M and E_{22}^S, leads to smaller κ and a lack of a κ_{env} dependence of the wave functions for the E_{33}^S and E_{44}^S excitons; (2) stronger tube screening (κ_{tube}) leads to an independence in κ_{env} and, consequently, a smaller effective κ.

In summary, we have shown that the diameter-dependent dielectric constants following Eq. (1) reproduce the measured E_{ii} values well for a large region of energy (1.2–2.7 eV) and tube diameter (0.7–3.8 nm). The present treatment for κ is sufficiently accurate for assigning both the $2n + m$ family numbers and the (n, m) SWNTs belonging to each family for different SWNT samples, for the super-growth and alcohol-assisted samples used for establishing the model system of this Letter. All the observed E_{ii} vs (n, m) values are now theoretically described within experimental precision, considering use of the extended-tight binding model along with many-body corrections plus a diameter-dependent dielectric constant κ, as established in the present work [Eq. (1)]. The empirical exponent 1.7 is not yet fully understood, and theoretical modeling considering the role of effective mass is under way. The results presented here are also consistent with the previously published empirical methodology of Ref. [3], and therefore provide the theoretical justification for it.

Having justified this empirical methodology, the findings of the present work have the following implications on taking account of environmental effects for fitting the measured d_t dependence of ω_{RBM} for an arbitrary experimental sample. Using the results of the empirical methodology of Ref. [3], the measured $\omega_{\text{RBM}}(d_t)$ for an arbitrary experimental sample is fitted to the formula

$$\omega_{\text{RBM}} = (227/d_t)\sqrt{1 + C_e * d_t^2}, \qquad (2)$$

where only a single parameter (C_e) is used to account for the observed d_t-dependent environmental effects. For the case of the super-growth SWNTs we have a fit to the E_{ii}^{exp} data for $C_e = 0$ [7], while for the alcohol-assisted sample, the fit is accomplished by $C_e = 0.057$. However, for an arbitrary sample measured in the laboratory, a least squares fit is made by the researchers themselves to determine the best fit value for C_e in Eq. (2) to their experimental data. In this way the results of this paper can be extended to yield a fit of $\omega_{\text{RBM}}(d_t)$ to arbitrary samples in a metrological sense, based on a single fitting parameter C_e to account for the experimental environmental effect measured for their sample by the resonance Raman effect.

P. T. A. and A. J. acknowledge financial support by FAPEMIG, Rede de pesquisa em nanotubos de carbono MCT/CNPq and AFOSR. M. S. D. acknowledges support from NSF grant DMR07-04197. K. S. is supported by a JSPS research grant (No. 20-4594). R. S. acknowledges support from MEXT Grants (No. 20241023).

[1] A. Jorio, M. S. Dresselhaus, and G. Dresselhaus, *Carbon Nanotubes: Advanced Topics in the Synthesis, Structure, Properties and Applications* Springer Series on Topics in Appl. Phys. 111 Vol. 111 (Springer-Verlag, Berlin, 2008).
[2] C. L. Kane, and E. J. Mele, Phys. Rev. Lett. **90**, 207401 (2003).
[3] P. T. Araujo *et al.*, Phys. Rev. Lett. **98**, 067401 (2007).
[4] T. Michel *et al.*, Phys. Rev. B **75**, 155432 (2007).
[5] K. Sato *et al.*, Phys. Rev. B **76**, 195446 (2007).
[6] J. Jiang *et al.*, Phys. Rev. B **75**, 035407 (2007).
[7] P. T. Araujo *et al.*, Phys. Rev. B **77**, 241403(R) (2008).
[8] P. T. Araujo and A. Jorio, Phys. Status Solidi B **245**, 2201 (2008).
[9] See EPAPS Document No. E-PRLTAO-103-022942 for an example of the resonant Raman spectral profile of the carpetlike water-assisted CVD grown SWNTs ranging from 65 cm^{-1} to 4550 cm^{-1}. In addition, file Epaps-Araujo-EiiKappaTable.xls brings the experimental ω_{RBM}, E_{ii} and the κ values fitting E_{ii} for the samples analyzed in our Letter. For the alcohol-assisted sample we present experimental results for 84 different (n, m) SWNTs, including E_{ii} values for E_{22}^S, E_{11}^M (lower branch), E_{33}^S and E_{44}^S. For the water-assisted sample we present experimental values for 176 different (n, m), including E_{ii} values for E_{11}^S, E_{22}^S, E_{11}^M (lower branch), E_{11}^M (higher branch), E_{33}^S, E_{44}^S, E_{22}^M (lower branch), E_{22}^M (higher branch), E_{55}^S and E_{66}^S. For more information on EPAPS, see http://www.aip.org/pubservs/epaps.html.
[10] K. Hata *et al.*, Science **306**, 1362 (2004).
[11] D. N. Futaba *et al.*, Phys. Rev. Lett. **95**, 056104 (2005).
[12] D. N. Futaba *et al.*, J. Phys. Chem. B **110**, 8035 (2006).
[13] D. N. Futaba *et al.*, Nature Mater. **5**, 987 (2006).
[14] S. K. Doorn, P. T. Araujo, K. Hata, and A. Jorio, Phys. Rev. B **78**, 165408 (2008).
[15] M. Milnera, J. Kürti, M. Hulman, and H. Kuzmany, Phys. Rev. Lett. **84**, 1324 (2000).
[16] S. M. Bachilo *et al.*, Science **298**, 2361 (2002).
[17] M. Y. Sfeir *et al.*, Science **312**, 554 (2006).
[18] S. K. Doorn *et al.*, Appl. Phys. A **78**, 1147 (2004).
[19] C. Fantini *et al.*, Phys. Rev. Lett. **93**, 147406 (2004).
[20] H. Telg *et al.*, Phys. Rev. Lett. **93**, 177401 (2004).
[21] A. Débarre *et al.*, Phys. Rev. Lett. **101**, 197403 (2008).
[22] Y. Miyauchi *et al.*, Chem. Phys. Lett. **442**, 394 (2007).
[23] V. Perebeinos, J. Tersoff, and Ph. Avouris, Phys. Rev. Lett. **92**, 257402 (2004).
[24] Y. Murakami, E. Einarsson, T. Edamura, and S. Maruyama, Carbon **43**, 2664 (2005).